

# $\Lambda(1405)$ -induced non-mesonic decay in kaonic nuclei

T. Sekihara, D. Jido<sup>1</sup>, and Y. Kanada-En'yo<sup>1</sup>

*Department of Physics, Kyoto University, Kyoto 606-8502, Japan and*

<sup>1</sup>*Yukawa Institute for Theoretical Physics, Kyoto University, Kyoto 606-8502, Japan*

(Dated: October 31, 2018)

Non-mesonic decay of kaonic nuclei is investigated under a  $\Lambda(1405)$  doorway picture where the  $\bar{K}$  absorptions in nuclei take place through the  $\Lambda(1405)$  resonance. Calculating  $\Lambda(1405)N \rightarrow YN$  transitions with one-meson exchange, we find that the non-mesonic decay ratio  $\Gamma_{\Lambda N}/\Gamma_{\Sigma^0 N}$  depends strongly on the ratio of the couplings  $\Lambda(1405)\text{-}\bar{K}N$  and  $\Lambda(1405)\text{-}\pi\Sigma$ . Especially a larger  $\Lambda(1405)\text{-}\bar{K}N$  coupling leads to enhancement of the decay to  $\Lambda N$ . Using the chiral unitary approach for description of the  $\bar{K}N$  amplitudes, we obtain  $\Gamma_{\Lambda N}/\Gamma_{\Sigma^0 N} \approx 1.2$  almost independently of the nucleon density, and find the total non-mesonic decay width calculated in uniform nuclear matter to be 22 MeV at the normal density.

PACS numbers: 21.85.+d, 14.20.Jn, 13.75.Jz, 13.30.Eg

Keywords: Non-mesonic decay, kaonic nuclei;  $\Lambda(1405)$  doorway;  $\Gamma_{\Lambda N}/\Gamma_{\Sigma^0 N}$  ratio; Chiral unitary approach

## I. INTRODUCTION

The in-medium properties of hadrons are key clues to understand finite density QCD. Meson-nucleus bound systems are good experimental objects to observe the in-medium properties of hadrons. Anti-kaon ( $\bar{K}$ ) bound states in nuclear systems (kaonic nuclei) are theoretically expected to exist due to strongly attractive interactions between the  $\bar{K}$  and nucleon [1–3]. In spite of experimental efforts to search for the  $\bar{K}$ -nuclear bound systems [4], there are no clear evidences observed yet.

For the observation of the kaonic nuclei in experiments, strength of  $\bar{K}$  absorptions is a key property. With smaller  $\bar{K}$  absorption widths than level spacings of the bound states, missing mass spectroscopy may be suitable to observe the kaonic bound states in kaon transfer reactions, such as ( $K^-$ ,  $N$ ) with nuclear targets [1] (see also Ref. [5]). For larger widths, coincident observations of particles emitted from the decay of the kaonic nuclei may be essential to pin down the  $\bar{K}$  bound states, and the decay patterns tell us the properties of the bound states.

The decay of the kaonic nuclei in strong interactions is categorized into two processes; one is the mesonic process such as  $\bar{K}N \rightarrow \pi Y$ , and the other is the non-mesonic process such as  $\bar{K}NN \rightarrow YN$ , where  $Y$  denotes hyperon ( $\Lambda$  or  $\Sigma$ ). The non-mesonic decays have advantage in experimental observations, since signals from kaonic nuclei are readily distinguished from backgrounds and no extra mesons do not have to be detected. Therefore, systematic studies of the non-mesonic decay of the kaonic nuclei are desirable. Especially the ratios of the decay widths are interesting, since they will be insensitive to details of the production mechanism.

The absorption of the  $\bar{K}$  in nuclei may take place dominantly through the  $\Lambda(1405)$  ( $\Lambda^*$ ) resonance, owing to the presence of the  $\Lambda^*$  just below the  $\bar{K}N$  threshold. Namely the  $\Lambda^*$  can be a doorway of the  $\bar{K}$  absorptions in nuclei. The  $\Lambda^*$  doorway picture is more probable, in case that the  $\Lambda(1405)$  is a quasi-bound state of  $\bar{K}N$  [6, 7], which has large  $\bar{K}N$  components as almost real particles.

Recently it has been reported based on the  $\bar{K}N$  quasi-bound picture of the  $\Lambda(1405)$  in Refs. [3, 8, 9] that also in few-body hadronic systems the  $\bar{K}N$  correlation is so strong as to cause the significant component of the  $\Lambda^*$  resonance. It has been also pointed out that the  $\Lambda^*$  as the  $\bar{K}N$  quasi-bound is not so compact compared with a typical hadronic size [3, 10]. Therefore the strong  $\bar{K}N$  correlations are expected to be responsible for the  $\Lambda^*$ -induced decays of the  $\bar{K}$  in nuclei.

In this paper, we study the non-mesonic decay of the kaonic nuclei under the  $\Lambda^*$ -induced picture, in which the decay process has the strong  $\bar{K}N$  correlation in its initial state. For this purpose, we calculate the  $\Lambda^*N \rightarrow YN$  process ( $\Lambda^*p \rightarrow \Lambda p, \Sigma^0 p, \Sigma^+ n$  and  $\Lambda^*n \rightarrow \Lambda n, \Sigma^0 n, \Sigma^- p$ ) in uniform nuclear matter with a one-meson exchange approach. We will see that the decay ratio  $\Gamma_{\Lambda N}/\Gamma_{\Sigma^0 N}$  depends strongly on  $s$ -wave  $\Lambda^*$  couplings to  $\bar{K}N$  and  $\pi\Sigma$ . Fixing the  $\Lambda^*$  couplings by the  $\bar{K}N$  scattering amplitudes calculated in the chiral unitary approach, we evaluate the non-mesonic decay widths of  $\Lambda^*$  in nuclear medium as functions of the nucleon density.

The non-mesonic decay widths of the  $\Lambda^*$  in nuclei are calculated by  $\Lambda^*N \rightarrow YN$ . In Sec. II, our formulation of the  $\Lambda^*N \rightarrow YN$  transition rate is explained. We show the ratio of the  $\Lambda^*N$  transitions to  $\Lambda N$  and  $\Sigma N$  as a function of the  $\Lambda^*$  couplings to  $\bar{K}N$  and  $\pi\Sigma$  in Sec. III. The non-mesonic decay widths are evaluated in nuclear matter as functions of the nucleon density in Sec. IV. Section V is devoted to a summary.

## II. FORMULATION OF $\Lambda^*N \rightarrow YN$ PROCESS

In this section, we formulate the  $\Lambda^*N \rightarrow YN$  transition process in a meson-exchange approach. Here  $N$  denotes  $p$  or  $n$ , and  $Y$  is  $\Lambda$  or  $\Sigma$ . The  $\Lambda^*N \rightarrow YN$  transition is a possible elementary process of the non-mesonic decay of the  $\bar{K}$  in nuclear medium. Summing up the  $\Lambda^*N \rightarrow YN$  transition rate in terms of the initial nucleon states, we estimate the non-mesonic decay width

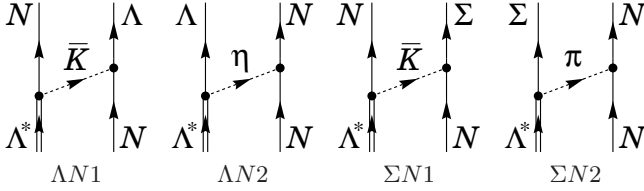


FIG. 1: Feynman diagrams for the  $\Lambda^* N \rightarrow Y N$  transition in the one-meson exchange model. The upper two diagrams are for the  $\Lambda N$  final state and the lower two are for the  $\Sigma N$  state.

of the  $\bar{K}$  in nuclear medium as a function of the nucleon density in Sec. IV.

The transition rate is given by the transition probability divided by time  $\mathcal{T}$  as

$$\gamma_{YN} \equiv \frac{1}{\mathcal{T}} \frac{1}{\mathcal{V}^2} \frac{1}{4} \sum_{\text{spin}} \int d\Phi_2 |S - 1|^2, \quad (1)$$

with the  $S$ -matrix  $S$  for the transition process given by the transition amplitudes  $T_{YN}$  as  $S = 1 - i(2\pi)^4 \delta^4(P_{\Lambda^*} + P_{\text{in}} - P_N - P_Y) T_{YN}$  and the energy-momenta,  $P_{\Lambda^*}$ ,  $P_{\text{in}}$  for the initial  $\Lambda^*$  and nucleon  $N$ , and  $P_Y$ ,  $P_N$  for the outgoing hyperon  $Y$  and nucleon  $N$ , respectively. The subscript “ $YN$ ” of  $\gamma_{YN}$  and  $T_{YN}$  represents the particles in the final state. The wavefunctions of the baryons have been introduced as plain waves normalized as unity in a spatial volume  $\mathcal{V}$ . We have taken spin summation for the final state and spin average for the initial state. The phase space  $d\Phi_2$  of the final state is given by

$$d\Phi_2 \equiv \frac{d^3 p_Y}{(2\pi)^3} \frac{2M_Y}{2E_Y} \frac{d^3 p_N}{(2\pi)^3} \frac{2M_N}{2E_N}, \quad (2)$$

with the normalization of the baryonic state as  $\langle \mathbf{p}_i | \mathbf{p}'_i \rangle = (2\pi)^3 2E_i \delta^3(\mathbf{p}_i - \mathbf{p}'_i) / (2M_i)$  and  $E_i = \sqrt{M_i^2 + \mathbf{p}_i^2}$ . The masses of the  $\Lambda^*$ , nucleon and hyperon are denoted by  $M_{\Lambda^*}$ ,  $M_N$  and  $M_Y$ , respectively. The transition rate depends on the center-of-mass energy  $E_{\text{c.m.}}$ , equivalently the initial nucleon momentum.

Performing the phase space integral in Eq. (1) in the  $\Lambda^*$  rest frame, we obtain

$$\gamma_{YN}(p_{\text{in}}) = \frac{1}{\mathcal{V}} \frac{1}{8\pi} \sum_{\text{spin}} \int_{-1}^1 d \cos \theta_N |T_{YN}|^2 \times \frac{p_N M_Y M_N}{E_Y + E_N - p_{\text{in}} \cos \theta_N E_N / p_N}, \quad (3)$$

where  $P_Y^\mu = (E_Y, \mathbf{p}_Y)$ ,  $P_N^\mu = (E_N, \mathbf{p}_N)$ ,  $P_{\text{in}}^\mu = (E_{\text{in}}, \mathbf{p}_{\text{in}})$  and  $\theta_N$  denotes the angle of  $\mathbf{p}_N$  to  $\mathbf{p}_{\text{in}}$ . We have used  $(2\pi)^4 \delta^4(0) = \mathcal{T}\mathcal{V}$ . The factor  $1/\mathcal{V}$  is responsible for the fact that only one  $N$  exists in the initial state in the volume  $\mathcal{V}$ . Later it will be interpreted as nuclear density in nuclear matter calculation. In the case that the  $\Lambda^*$  and  $N$  interact in the initial state, the factor  $1/\mathcal{V}$  for the plain-wave should be replaced by the square of a relative wavefunction of the two-body  $\Lambda^* N$  system.

We evaluate the transition amplitudes  $T_{YN}$  with one-meson exchange diagrams shown in Fig. 1. This approach

of non-mesonic decay calculation with the one-meson exchange diagrams was applied for  $\Lambda$  hypernuclei, reproducing the experimental values of the ratios  $\Gamma_n/\Gamma_p$  for wide range of hypernuclei well [11]. We assume isospin symmetry, thus the transition amplitudes  $T_{YN}$  are independent from type of the nucleons in the initial state because the  $\Lambda^*$  has isospin  $I = 0$ .

The transition amplitudes with the  $\Lambda N$  and  $\Sigma^0 N$  in the final state can be written in terms of two parts corresponding to the exchanged meson:

$$T_{\Lambda N} \equiv T_{\Lambda N1} - T_{\Lambda N2}, \quad (4)$$

$$T_{\Sigma^0 N} \equiv T_{\Sigma^0 N1} - T_{\Sigma^0 N2}, \quad (5)$$

where the indices ( $\Lambda N1$  etc.) are given in Fig. 1. The relative sign between two amplitudes comes from exchange of  $Y$  and  $N$  in the final state. The amplitude  $T_{Y\pm N}$  can be obtained by the isospin relation:  $T_{Y\pm N} = \sqrt{2} T_{\Sigma^0 N}$ .

Each amplitude of the diagrams given in Fig. 1 is evaluated by introducing  $s$ -wave  $\Lambda^* M B$  coupling constants  $G_{MB}$ ,  $M B B$  interactions  $V_{M B B}$  and meson propagators  $\Pi_M(q_M^2)$  ( $M$  and  $B$  represent the mesons and baryons in the particle-basis, respectively) as

$$T_{\Lambda N1} = G_{\bar{K} N} \Pi_{\bar{K}}(q_{\bar{K}}^2) V_{\bar{K} N \Lambda}, \quad (6)$$

$$T_{\Lambda N2} = G_{\eta \Lambda} \Pi_{\eta}(q_{\eta}^2) V_{\eta N N}, \quad (7)$$

for the  $\Lambda N$  final state, and

$$T_{\Sigma^0 N1} = G_{\bar{K} N} \Pi_{\bar{K}}(q_{\bar{K}}^2) V_{\bar{K} N \Sigma^0}, \quad (8)$$

$$T_{\Sigma^0 N2} = G_{\pi \Sigma} \Pi_{\pi}(q_{\pi}^2) V_{\pi^0 N N}, \quad (9)$$

for the  $\Sigma^0 N$  final state. Because of the isospin symmetry, we have  $G_{\bar{K} N} = G_{K^- p} = G_{\bar{K}^0 n}$  and  $G_{\pi \Sigma} = G_{\pi^0 \Sigma^0} = G_{\pi^\pm \Sigma^\mp}$ .

The  $s$ -wave  $\Lambda^* M B$  coupling constants  $G_{MB}$  are determined by the properties of the  $\Lambda^*$ . In the present work, first we treat  $G_{MB}$  as model parameters, and later we fix them from the chiral unitary approach, which reproduces the  $\Lambda^*$  in meson-baryon dynamics.

The meson-baryon-baryon three-point interactions  $V_{M B B}$  are obtained from the low energy theorem in the flavor SU(3) symmetry. The interaction Lagrangian is written as

$$\mathcal{L}_{\text{int}} = -\frac{D+F}{\sqrt{2}f} \langle \bar{B} \gamma^\mu \gamma^5 \partial_\mu \Phi B \rangle - \frac{D-F}{\sqrt{2}f} \langle \bar{B} \gamma^\mu \gamma^5 B \partial_\mu \Phi \rangle, \quad (10)$$

where  $D$  and  $F$  are the low energy constants which cannot be determined by the flavor symmetry, and  $f$  is the meson decay constant. We use empirical values of  $D + F = g_A = 1.26$  and  $D - F = 0.33$ , which reproduce the hyperon  $\beta$  decays observed in experiment, and  $f = f_\pi = 93.0 \text{ MeV}$  commonly for all the mesons. The matrices  $B$  and  $\Phi$  are the SU(3) expressions of the baryon and meson fields, respectively. From the Lagrangian (10), we obtain the  $p$ -wave  $M B B$  interactions in non-relativistic limit:

$$-iV_{M B B} = -\frac{d_{M B B} D + f_{M B B} F}{f} \mathbf{q}_M \cdot \boldsymbol{\sigma}, \quad (11)$$

with the incoming meson momentum  $\mathbf{q}_M$ , Pauli matrices  $\boldsymbol{\sigma}$  for baryon spin and the SU(3) Clebsch-Gordan coefficients  $d_{MBB}$  and  $f_{MBB}$ .

The propagator  $\Pi_M(q_M^2)$  for the meson  $M$  is given by

$$\Pi_M(q_M^2) \equiv \frac{1}{q_M^2 - m_M^2}. \quad (12)$$

The exchange meson momenta,  $q_\pi^\mu$  for  $\pi$ ,  $q_\eta^\mu$  for  $\eta$  and  $q_{\bar{K}}^\mu$  for  $\bar{K}$ , are fixed kinematically as

$$q_\pi^\mu = q_\eta^\mu = P_{\Lambda^*}^\mu - P_Y^\mu, \quad q_{\bar{K}}^\mu = P_{\Lambda^*}^\mu - P_N^\mu. \quad (13)$$

In our study we take into account the short-range correlation, which compensates the short-range behavior of the meson-exchange potential [12]. This can be introduced by changing the meson propagators to

$$\Pi(q^2) \rightarrow \tilde{\Pi}(q^2) \equiv \Pi(q^2)[F(q^2)]^2 - \Pi(\tilde{q}^2)[F(\tilde{q}^2)]^2, \quad (14)$$

with the mono-pole form factor  $F(q^2) = \frac{\Lambda^2}{\Lambda^2 - q^2}$  and  $\tilde{q}^2 = q^2 - q_C^2$ . We choose typical parameter set,  $\Lambda = 1.0$  GeV and  $q_C = 780$  MeV [11].

### III. RATIO OF TRANSITION RATES – GENERAL PROPERTIES

In the previous section, we have obtained the transition rates of  $\Lambda^*N \rightarrow YN$  in Eq. (3) together with the transition amplitudes (6)-(9) in the one-meson exchange model. In the present calculation, the  $MBB$  interactions  $V_{MBB}$  are fixed by the flavor SU(3) symmetry with the empirical values of  $D$  and  $F$ , while the  $\Lambda^*MB$  coupling constants  $G_{MB}$  are to be determined by the properties of the  $\Lambda^*$ . In this section, we discuss  $G_{MB}$  coupling dependence of the ratio of the transition rates to  $\Lambda N$  and  $\Sigma^0 N$ ,  $\gamma_{\Lambda N}/\gamma_{\Sigma^0 N}$ .

First of all, it is helpful for understanding of the  $\Lambda^*N \rightarrow YN$  transition rates to see which diagrams out of four shown in Fig. 1 dominate the transition rates. For this purpose, we show the  $MBB$  coupling constants obtained by the low energy theorem with the present parameter  $F$  and  $D$ :

$$V_{\bar{K}N\Lambda} \propto \frac{D+3F}{2\sqrt{3}} \simeq 0.63, \quad V_{\eta NN} \propto \frac{D-3F}{2\sqrt{3}} \simeq -0.10,$$

$$V_{\bar{K}N\Sigma^0} \propto \frac{D-F}{2} \simeq 0.17, \quad V_{\pi^0 NN} \propto \frac{D+F}{2} \simeq 0.63.$$

These numbers indicate that the diagrams  $\Lambda N1$  and  $\Sigma N2$  give dominant contributions to the transition rates, while the diagram  $\Lambda N2$ , in which the  $\eta$  meson is exchanged, and the  $\Sigma N1$  diagram are much less important with factors  $1/6$  and  $1/4$  in the amplitudes than the dominant diagrams. Thus, the  $\bar{K}$  exchange is important in the  $\Lambda^*N \rightarrow \Lambda N$  transition, whereas the  $\pi$  exchange gives a dominant contribution in  $\Lambda^*N \rightarrow \Sigma N$ .

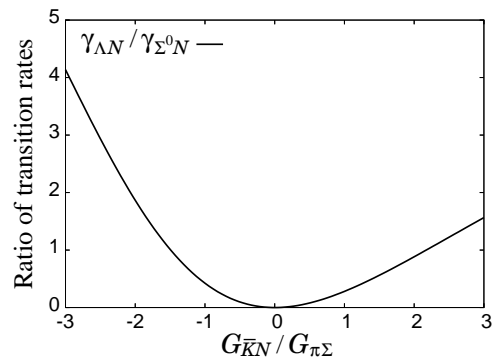


FIG. 2: Ratio of the transition rates of  $\Lambda^*N$  to  $\Lambda N$  and  $\Sigma^0 N$ ,  $\gamma_{\Lambda N}/\gamma_{\Sigma^0 N}$ , as a function of  $G_{\bar{K}N}/G_{\pi\Sigma}$ . We fix the initial nucleon momentum  $p_{\text{in}} = 0$  and the  $\Lambda^*$  mass  $M_{\Lambda^*} = 1420$  MeV and assume  $G_{\eta\Lambda} = 0$ .

Let us calculate the ratio of the transition rates,  $\gamma_{\Lambda N}/\gamma_{\Sigma^0 N}$ . Here we assume  $G_{\eta\Lambda} = 0$ , since the  $\eta NN$  coupling is negligible due to the small  $\eta NN$  coupling. Thus the ratio  $\gamma_{\Lambda N}/\gamma_{\Sigma^0 N}$  becomes a function of  $G_{\bar{K}N}/G_{\pi\Sigma}$ . We set also the initial nucleon momentum  $p_{\text{in}} = 0$  and the  $\Lambda^*$  mass  $M_{\Lambda^*} = 1420$  MeV<sup>1</sup>. Nevertheless, the transition rates are insensitive to  $p_{\text{in}}$  and  $M_{\Lambda^*}$ , because the phase space of the  $\Lambda^*N \rightarrow YN$  transition is sufficiently large against certain changes of  $p_{\text{in}}$  and  $M_{\Lambda^*}$ , for instance, to  $p_{\text{in}} \approx 300$  MeV and  $M_{\Lambda^*} \approx 1400$  MeV.

In Fig. 2, we show the numerical result of the ratio of the transition rates,  $\gamma_{\Lambda N}/\gamma_{\Sigma^0 N}$ , as a function of  $G_{\bar{K}N}/G_{\pi\Sigma}$ , in which we assume  $G_{\bar{K}N}/G_{\pi\Sigma}$  to be a real number. As seen in the figure, the ratio  $\gamma_{\Lambda N}/\gamma_{\Sigma^0 N}$  has strong dependence on the coupling ratio  $G_{\bar{K}N}/G_{\pi\Sigma}$ . This is because the transition to  $\Lambda N$  is governed by the  $\bar{K}$  exchange and the transition to  $\Sigma N$  is dominated by the  $\pi$  exchange. This result suggests that larger  $\Lambda^*\bar{K}N$  coupling leads to enhancement of the decay ratio to  $\Lambda N$  in the kaonic nuclei, although the  $\Lambda^*$  in vacuum cannot decay into final states including  $\Lambda$ .

The asymmetric behavior of the ratio of the transition rates under change of the sign of the coupling ratio comes from interference between the diagrams  $\Sigma N1$  and  $\Sigma N2$ .  $\Sigma N1$  gives subdominant contributions to  $\gamma_{\Sigma N}$  and depends on  $G_{\bar{K}N}$ . If the relative sign of  $G_{\bar{K}N}$  and  $G_{\pi\Sigma}$  is negative, the diagrams  $\Sigma N1$  and  $\Sigma N2$  are summed destructively. Thus, the ratio  $\gamma_{\Lambda N}/\gamma_{\Sigma^0 N}$  for  $G_{\bar{K}N}/G_{\pi\Sigma} < 0$  is larger than the corresponding ratio with  $G_{\bar{K}N}/G_{\pi\Sigma} > 0$ .

Finally it is worth noting again that the ratio of the transition rates is insensitive to the mass shift of the  $\Lambda^*$ . This means that, even in the case of in-medium modification of the  $\Lambda^*$  mass, as long as the  $\Lambda^*$  resonance is predominant in the  $\bar{K}N$  channel, the enhancement of the

<sup>1</sup> The chiral unitary model suggests that the resonance position of the  $\Lambda(1405)$  in the  $\bar{K}N$  channel is 1420 MeV instead of 1405 MeV and its width is 40 MeV, which is consistent with experimental data [13]. See Ref. [14, 15] for details.

decay to  $\Lambda N$  in the kaonic nuclei stems from larger coupling of the  $\Lambda^*$  to  $\bar{K}N$ . It is also noted that, even if the coupling constants  $G_{\bar{K}N}$  and  $G_{\pi\Sigma}$  are complex numbers, one can obtain a similar behavior for  $|G_{\bar{K}N}/G_{\pi\Sigma}|$ , because the ratio of the transition rates is dominated by the two diagrams,  $\Lambda N1$  and  $\Sigma N2$ , which cannot interfere.

#### IV. NON-MESONIC DECAY WIDTH OF $\Lambda^*$ IN NUCLEAR MEDIUM

We calculate the non-mesonic decay of the  $\bar{K}$  in uniform nuclear matter induced by the  $\Lambda^*N \rightarrow YN$  transition ( $N = p$  or  $n$ ), under the free Fermi gas approximation for nuclear matter in which non-interacting nucleons fill the momentum states up to the Fermi momentum  $k_F$ . Assuming that the  $\Lambda^*$  is at rest in nuclear medium, we evaluate the non-mesonic decay width by summing up the transition rate of  $\Lambda^*N \rightarrow YN$  for all the pair of the  $\Lambda^*$  and the nucleons in a unit volume  $\mathcal{V}$ :

$$\Gamma_{YN} \equiv \sum_{i=1}^{A_N} \gamma_{YN}(k_i), \quad (15)$$

where  $A_N$  ( $N = p$  or  $n$ ) is the numbers of the protons or neutrons in  $\mathcal{V}$  given by the Fermi momentum  $k_{FN}$  as

$$A_N = \frac{k_{FN}^3}{3\pi^2} \mathcal{V}. \quad (16)$$

The proton and neutron densities are given by  $\rho_N \equiv k_{FN}^3/(3\pi^2)$ . With the explicit expression of  $\gamma_{YN}$  given in Eq. (3) and replacing the summation over the nucleon numbers to integral with respect to the nucleon momentum, we obtain

$$\begin{aligned} \Gamma_{YN} = & \int_0^{k_{FN}} dk \frac{k^2}{8\pi^3} \sum_{\text{spin}} \int_{-1}^1 d \cos \theta_N |T_{YN}|^2 \\ & \times \frac{p_N M_Y M_N}{E_Y + E_N - k \cos \theta_N E_N / p_N}. \end{aligned} \quad (17)$$

Here we note that, in the two-nucleon absorption of the  $\bar{K}$ , the emitted nucleon is not affected by Pauli blocking in nuclear medium, since the outgoing nucleon momentum is about 500 MeV in the  $\Lambda^*$ -rest frame, which is much larger than the Fermi momentum for the nuclear saturation density.

In the previous section, we have regarded the  $\Lambda^*$  couplings  $G_{MB}$  as free parameters. Here we estimate the  $\Lambda^*MB$  coupling constants by the  $s$ -wave  $\bar{K}N$  scattering amplitudes with  $I = 0$  around the  $\Lambda^*$  resonance energy, which are dominated by the  $\Lambda^*$  contribution initiated by  $\bar{K}N$ . Since the scattering amplitudes have the  $\Lambda^*$  propagator and the initial  $\bar{K}N \rightarrow \Lambda^*$  coupling, we take the ratios of the amplitudes to cancel out the propagator and the coupling for the extraction of the  $\Lambda^*MB$  couplings:

$$\frac{G_{\bar{K}N}}{G_{\pi\Sigma}} = \frac{t_{\bar{K}N}(W)}{t_{\pi\Sigma}(W)}, \quad \frac{G_{\bar{K}N}}{G_{\eta\Lambda}} = \frac{t_{\bar{K}N}(W)}{t_{\eta\Lambda}(W)}, \quad (18)$$

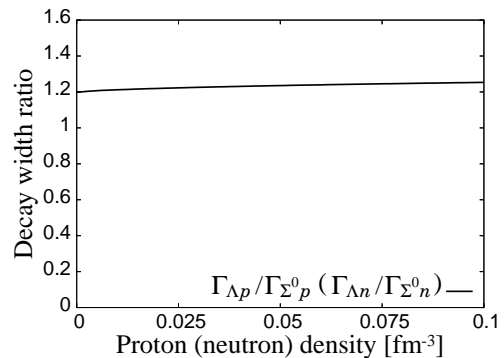


FIG. 3: Non-mesonic decay width ratio of kaonic nuclei.

where  $t_{MB}(W)$  is the scattering amplitude of  $\bar{K}N(I = 0)$  to  $MB$ (particle-basis) with the center-of-mass energy  $W$  chosen to be the  $\Lambda^*$  resonance position on the real energy axis.

For the description of the  $\bar{K}N$  scattering amplitudes  $t_{MB}(W)$ , we use the chiral unitary approach (ChUA), which reproduces well the  $s$ -wave scattering amplitudes of  $\bar{K}N \rightarrow MB$  in the coupled-channels method based on chiral dynamics and in which the  $\Lambda^*$  resonance is dynamically generated in the meson-baryon scattering. The model parameters of ChUA are determined so as to reproduce the threshold properties of  $K^-p$  observed in  $K^-$  absorptions of kaonic hydrogen [16, 17]. The details are given in Ref. [10], which is based on Refs. [18, 19]. Since the  $\Lambda^*$  resonance position in the  $\bar{K}N$  channel is 1420 MeV in ChUA, we take  $W = M_{\Lambda^*} = 1420$  MeV in Eq. (18). In the present work, we use the  $\bar{K}N$  scattering amplitude obtained in vacuum. Extensions with in-medium  $\Lambda^*$  modification are straightforward, as long as the  $\Lambda^*$  doorway picture of the  $\bar{K}$  absorption is valid in nuclear media. In-medium  $\Lambda^*$  coupling constants can be obtained through Eq. (18) with in-medium  $\bar{K}N$  scattering amplitudes as calculated, for instance, in Ref. [20].

Fixing the ratios of the  $\Lambda^*$  coupling constants,  $G_{MB}$ , we plot the ratio of the non-mesonic decay widths of the in-medium  $\bar{K}$  to  $\Lambda N$  and  $\Sigma^0 N$  as a function of the proton (or neutron) density in Fig. 3. This figure shows that the ratio of the non-mesonic decay widths  $\Gamma_{\Lambda N}/\Gamma_{\Sigma^0 N}$  is around 1.2 almost independently of the nucleon density. The value  $\Gamma_{\Lambda N}/\Gamma_{\Sigma^0 N} \approx 1.2$  is a consequence of the larger  $\Lambda^*$  coupling to  $\bar{K}N$  than  $\pi\Sigma$ . In ChUA, the ratio of the couplings  $|G_{\bar{K}N}/G_{\pi\Sigma}|$  is obtained as 2.5. The density independence of the ratio of the decay widths is due to the small dependence of the transition rate on the initial nucleon momentum, which is caused by sufficiently large phase space in the final states. It is worth noting that the ratios of the decay width will be insensitive to details of the production mechanism of the kaonic bound state, since they will be cancelled out.

To obtain absolute values of the non-mesonic decay width in nuclear matter, we use the mesonic decay width to  $\pi\Sigma$  as a reference:

$$\Gamma_{\Lambda^* \rightarrow \pi\Sigma} = 3 \times \frac{p_{\text{CM}} M_{\Sigma}}{2\pi M_{\Lambda^*}} |G_{\pi\Sigma}|^2, \quad (19)$$

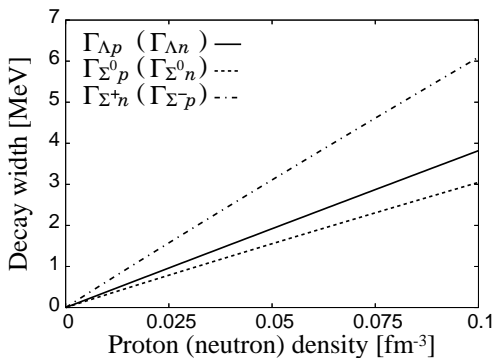


FIG. 4: Non-mesonic decay width of kaonic nuclei.

where  $p_{\text{CM}}$  is the center-of-mass momentum of  $\pi$ . Taking the mesonic decay width being  $\Gamma_{\Lambda^* \rightarrow \pi \Sigma} = 40$  MeV with  $M_{\Lambda^*} = 1420$  MeV as observed in a  $K^-$  initiated channel in vacuum [13, 15], we obtain  $|G_{\pi \Sigma}| = 0.78$ . The  $G_{\pi \Sigma}$  can be evaluated also within ChUA as  $|G_{\pi \Sigma}|_{\text{ChUA}} = 0.78$  on the real axis using the Breit-Wigner formula, and  $|G_{\pi \Sigma}|_{\text{pole}} = 0.88$  at the  $\Lambda^*$  complex pole position [14].

We show the non-mesonic decay widths calculated in nuclear medium,  $\Gamma_{\Lambda N}$ ,  $\Gamma_{\Sigma^0 N}$  and  $\Gamma_{\Sigma^\pm N}$ , in Fig. 4. The  $\Lambda^*$  couplings are determined by Eq. (18) with the ChUA amplitudes, and are normalized by Eq. (19) with  $\Gamma_{\Lambda^* \rightarrow \pi \Sigma} = 40$  MeV. The linear dependence of the decay widths is caused by insensitivity of the elementary transition rate  $\gamma_{YN}$  to the nucleon momentum. At the normal nuclear density ( $\rho_B = 0.17 \text{ fm}^{-3}$ ), the total non-mesonic decay width is 22 MeV, in which  $\Gamma_{\Lambda p} + \Gamma_{\Lambda n} = 7$  MeV,  $\Gamma_{\Sigma^0 p} + \Gamma_{\Sigma^0 n} = 5$  MeV and  $\Gamma_{\Sigma^+ n} + \Gamma_{\Sigma^- p} = 10$  MeV. This is almost half of the mesonic decay width of  $\Lambda^*$  ( $\sim 40$  MeV).

## V. CONCLUSION

We have investigated the non-mesonic decay of kaonic nuclei under the  $\Lambda(1405)$  doorway picture in which the  $\bar{K}$  absorption in nuclear medium takes place via the  $\Lambda^*$  resonance through  $\bar{K}N \rightarrow \Lambda^*$ . Calculating the  $\Lambda^*N \rightarrow YN$  transition rates in the one-meson exchange processes, we have found that the transition rate to  $\Lambda N$  is governed by the  $\bar{K}$  exchange, and consequently the ratio of the  $\Lambda^*N$  transition rates to  $\Lambda N$  and  $\Sigma N$  strongly depends on the ratio of the  $\Lambda^*$  couplings,  $G_{\bar{K}N}/G_{\pi \Sigma}$ . Particularly, larger  $\Lambda^*$  couplings to  $\bar{K}N$  lead to enhancement of the non-mesonic two-body  $\bar{K}$  absorption with  $\Lambda N$  emission.

Evaluating the  $\Lambda^*$  couplings by the  $\bar{K}N$  scattering amplitudes obtained by the chiral unitary approach, we have calculated the widths of the non-mesonic decay of kaonic nuclei induced by  $\Lambda^*N \rightarrow YN$ . We have obtained the ratio of the non-mesonic decay widths to  $\Lambda N$  and  $\Sigma^0 N$  as  $\Gamma_{\Lambda N}/\Gamma_{\Sigma^0 N} = 1.2$  almost independently of the nucleon density. We have also estimated that the total non-mesonic decay width is 22 MeV at the saturation density. These findings will help us to understand the properties of the kaonic nuclei.

## Acknowledgments

We would like to thank Dr. Fujioka for useful discussions. This work was supported in part by the Grant-in-Aid for Scientific Research from MEXT and JSPS (Nos. 18540263, 20028004 and 20540273), and the Grant-in-Aid for the Global COE Program "The Next Generation of Physics, Spun from Universality and Emergence" from MEXT of Japan. This work was done under the Yukawa International Program for Quark-hadron Sciences.

- 
- [1] T. Kishimoto, Phys. Rev. Lett. **83**, 4701 (1999).
  - [2] E. Friedman and A. Gal, Phys. Lett. **B459**, 43 (1999).
  - [3] Y. Akaishi and T. Yamazaki, Phys. Rev. **C65**, 044005 (2002); T. Yamazaki and Y. Akaishi, Proc. Japan Acad. **B83**, 144 (2007).
  - [4] T. Kishimoto et al., Prog. Theor. Phys. Suppl. **149**, 264 (2003); M. Agnello et al. (FINUDA), Phys. Rev. Lett. **94**, 212303 (2005); T. Kishimoto et al., Nucl. Phys. **A754**, 383 (2005); T. Suzuki et al., *ibid.* **A754**, 375 (2005).
  - [5] J. Yamagata and S. Hirenzaki, Eur. Phys. J. **A31**, 255 (2007); J. Yamagata, H. Nagahiro, and S. Hirenzaki, Phys. Rev. **C74**, 014604 (2006).
  - [6] R. H. Dalitz, T. C. Wong, and G. Rajasekaran, Phys. Rev. **153**, 1617 (1967).
  - [7] T. Hyodo, D. Jido, and A. Hosaka, Phys. Rev. **C78**, 025203 (2008).
  - [8] Y. Kanada-En'yo and D. Jido, Phys. Rev. **C78**, 025212 (2008); D. Jido and Y. Kanada-En'yo, *ibid.* **C78**, 035203 (2008).
  - [9] A. Dote, T. Hyodo, and W. Weise, Phys. Rev. **C79**, 014003 (2009).
  - [10] T. Sekihara, T. Hyodo, and D. Jido, Phys. Lett. **B669**, 133 (2008).
  - [11] D. Jido, E. Oset, and J. E. Palomar, Nucl. Phys. **A694**, 525 (2001).
  - [12] E. Oset and W. Weise, Nucl. Phys. **A319**, 477 (1979).
  - [13] O. Braun et al., Nucl. Phys. **B129**, 1 (1977).
  - [14] D. Jido, J. A. Oller, E. Oset, A. Ramos, and U. G. Meissner, Nucl. Phys. **A725**, 181 (2003).
  - [15] D. Jido, E. Oset, and T. Sekihara, arXiv:0904.3410 [nucl-th].
  - [16] D. N. Tovee et al., Nucl. Phys. **B33**, 493 (1971).
  - [17] R. J. Nowak et al., Nucl. Phys. **B139**, 61 (1978).
  - [18] E. Oset, A. Ramos, and C. Bennhold, Phys. Lett. **B527**, 99 (2002).
  - [19] T. Hyodo, S. I. Nam, D. Jido, and A. Hosaka, Phys. Rev. **C68**, 018201 (2003); Prog. Theor. Phys. **112**, 73 (2004).
  - [20] T. Waas, N. Kaiser, and W. Weise, Phys. Lett. **B365**, 12 (1996); M. Lutz, *ibid.* **B426**, 12 (1998); A. Ramos and E. Oset, Nucl. Phys. **A671**, 481 (2000).